



半導體奈米結構之成長與光電特性

交通大學電子物理系 周武清 教授

大綱:

Part I: 半導體奈米結構成長-----

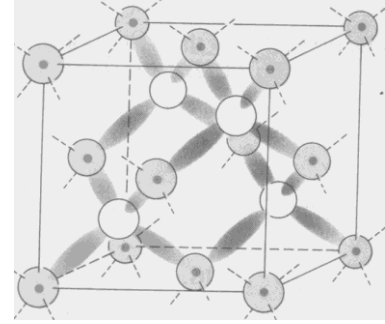
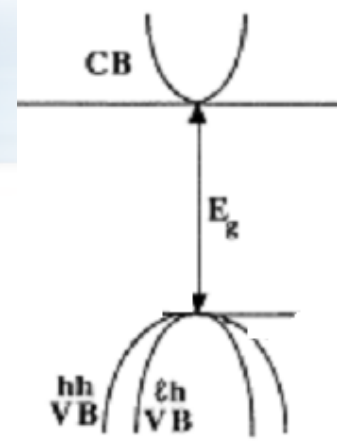
分子束磊晶(MBE, molecular beam epitaxy)

半導體奈米結構形貌研究---AFM

Part II: 半導體奈米結構光電特性---Photoluminescence

Part III: 半磁性半導體奈米結構之自旋磁光特性

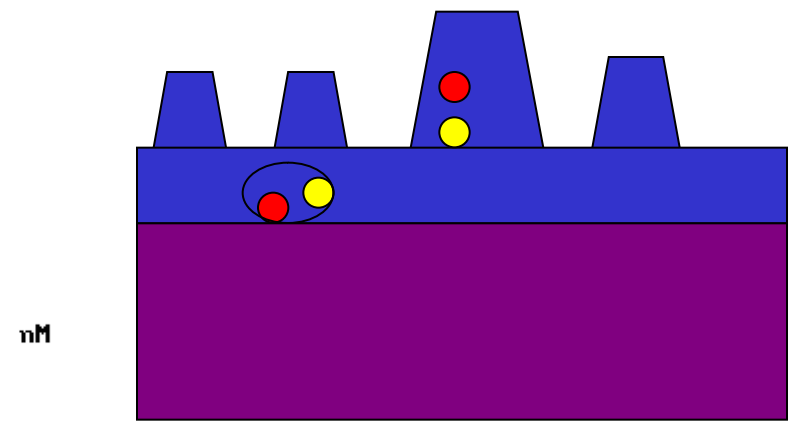
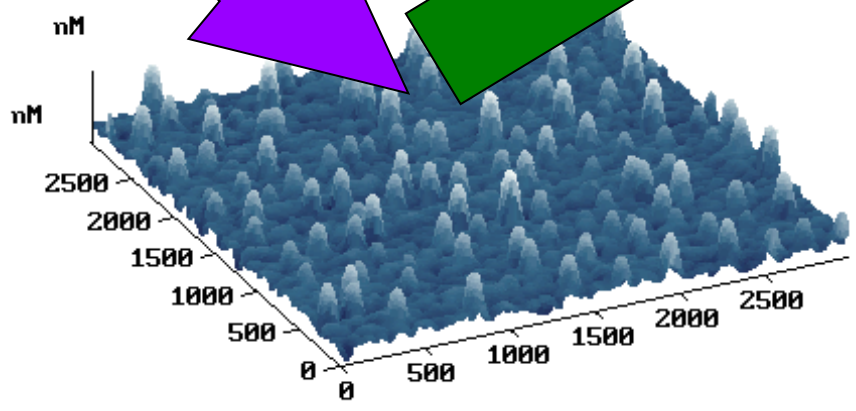




Pulse laser

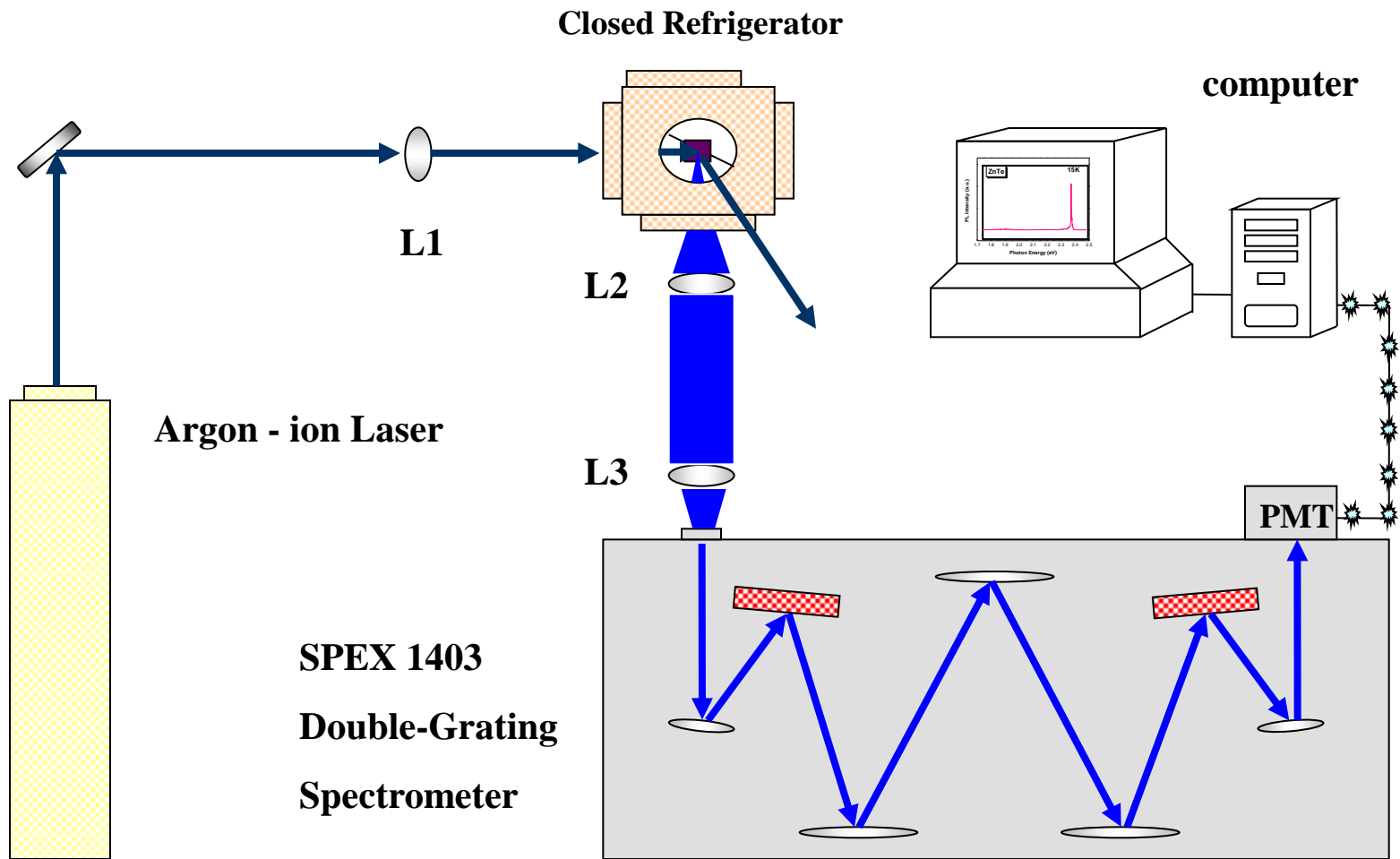
Excitation He-Cd laser 325 nm

Photoluminescence, PL
光激螢光



激子(exciton): 電子-電洞對

Photoluminescence (PL)

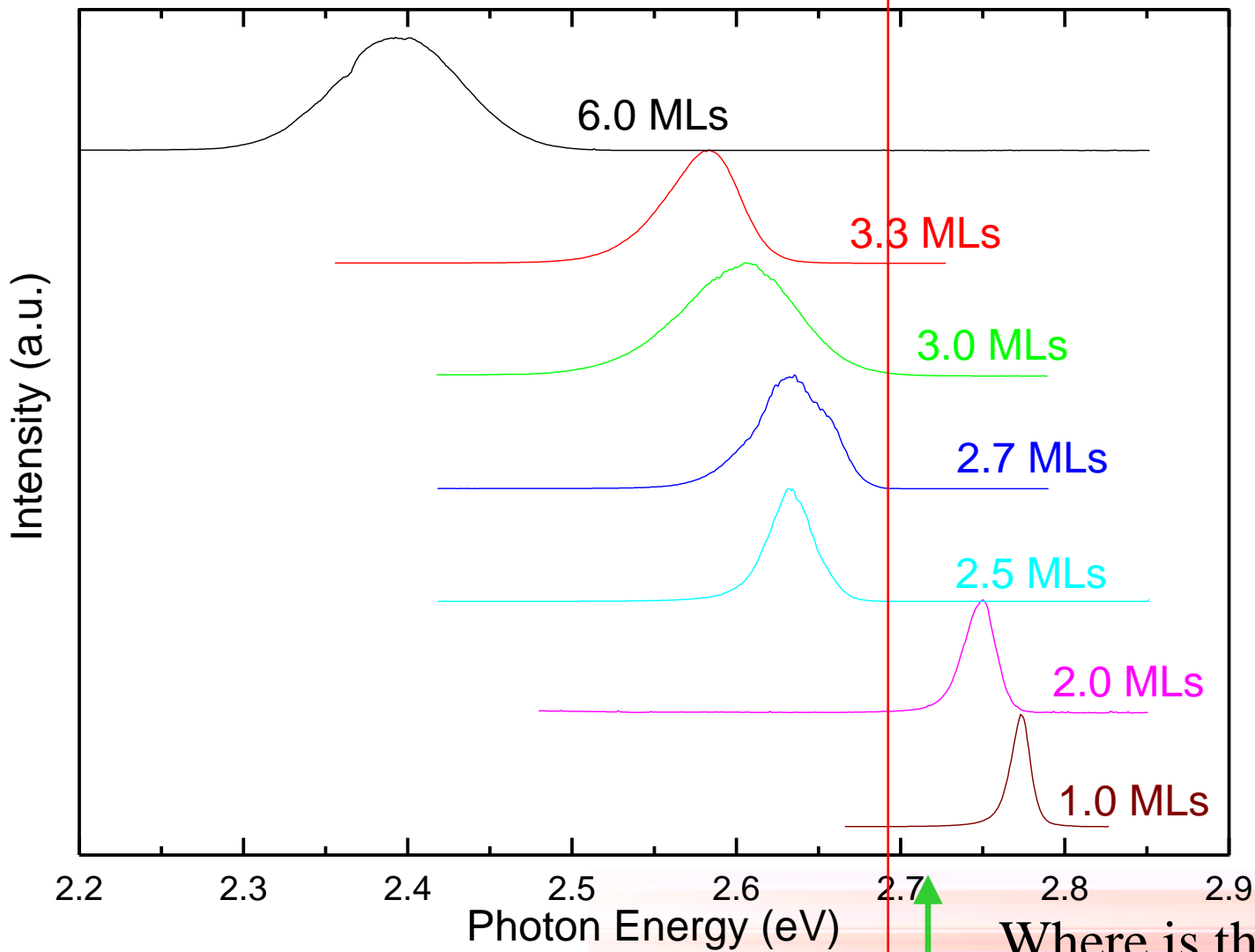




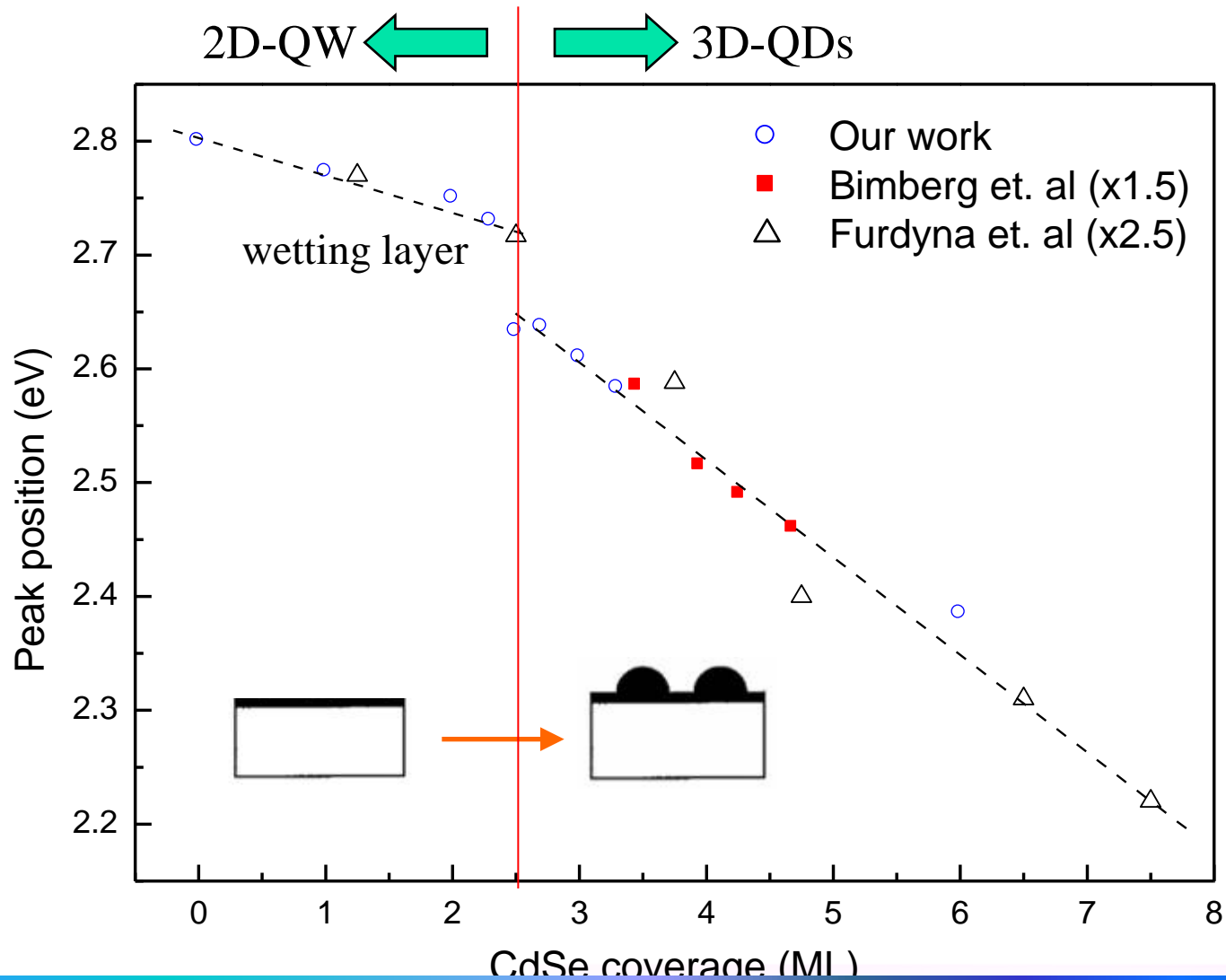
3D-QDs

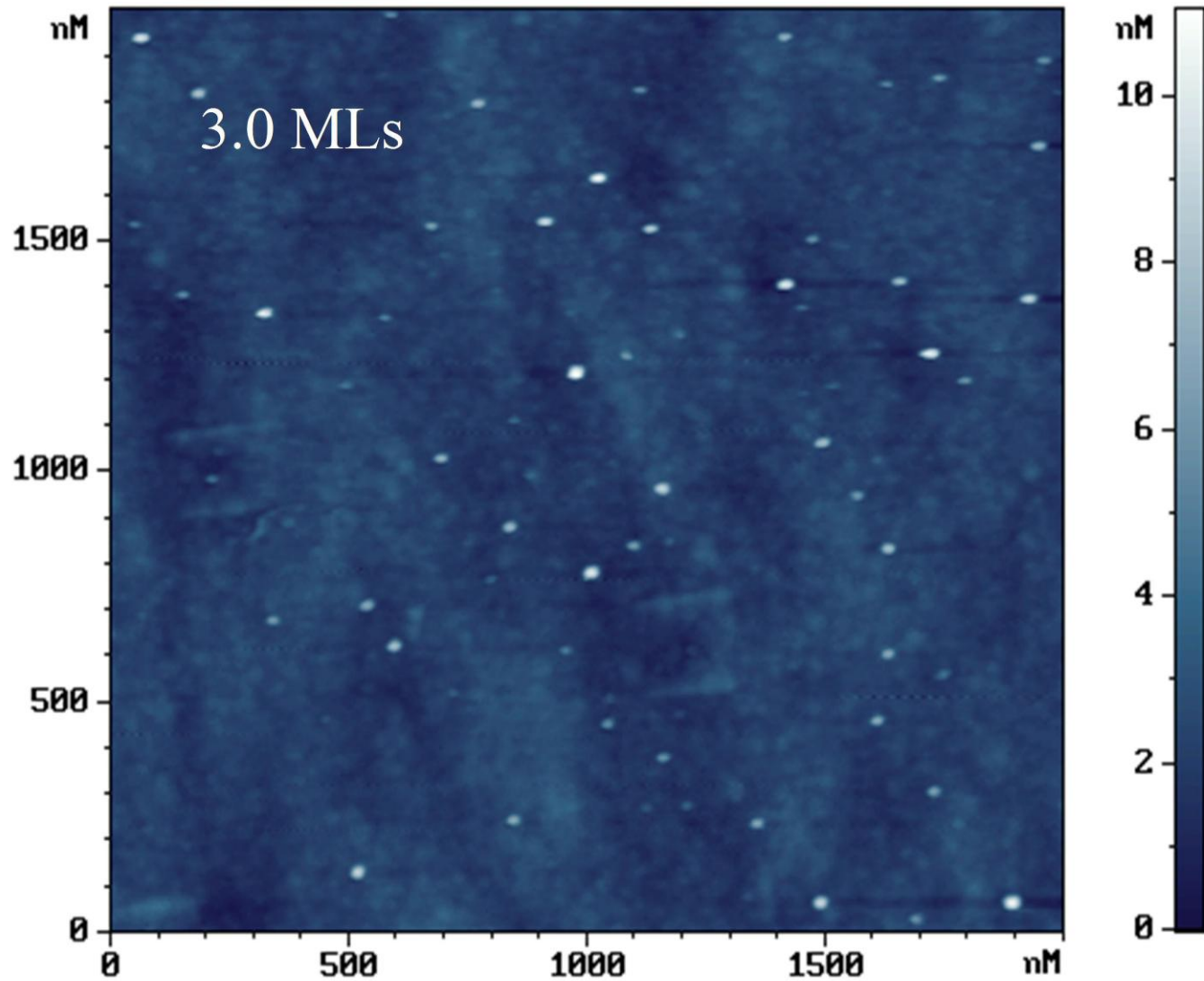
S-K

2D-QW



Peak position vs. CdSe coverage :

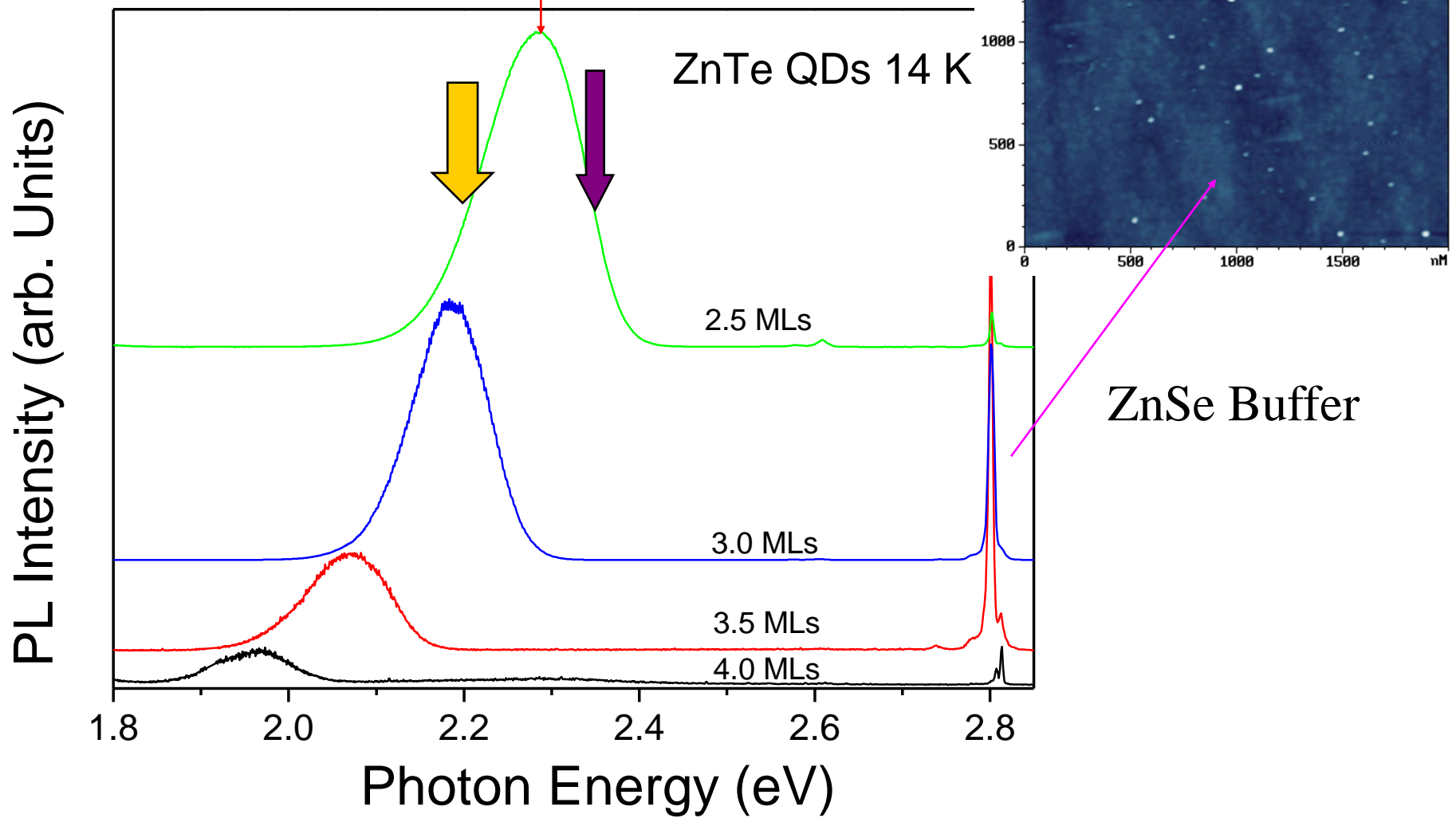




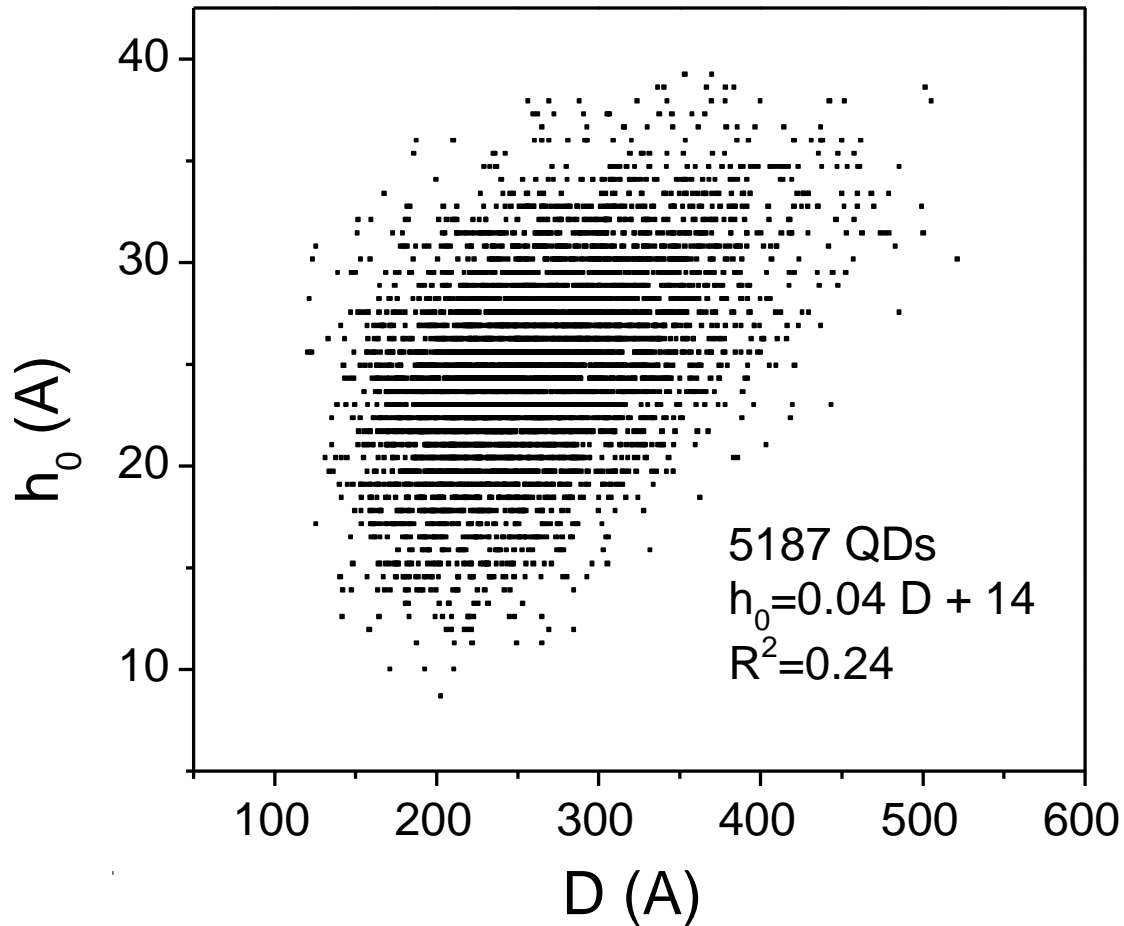
The top-view AFM image of the ZnTe QDs with coverage of 3.0 MLs.



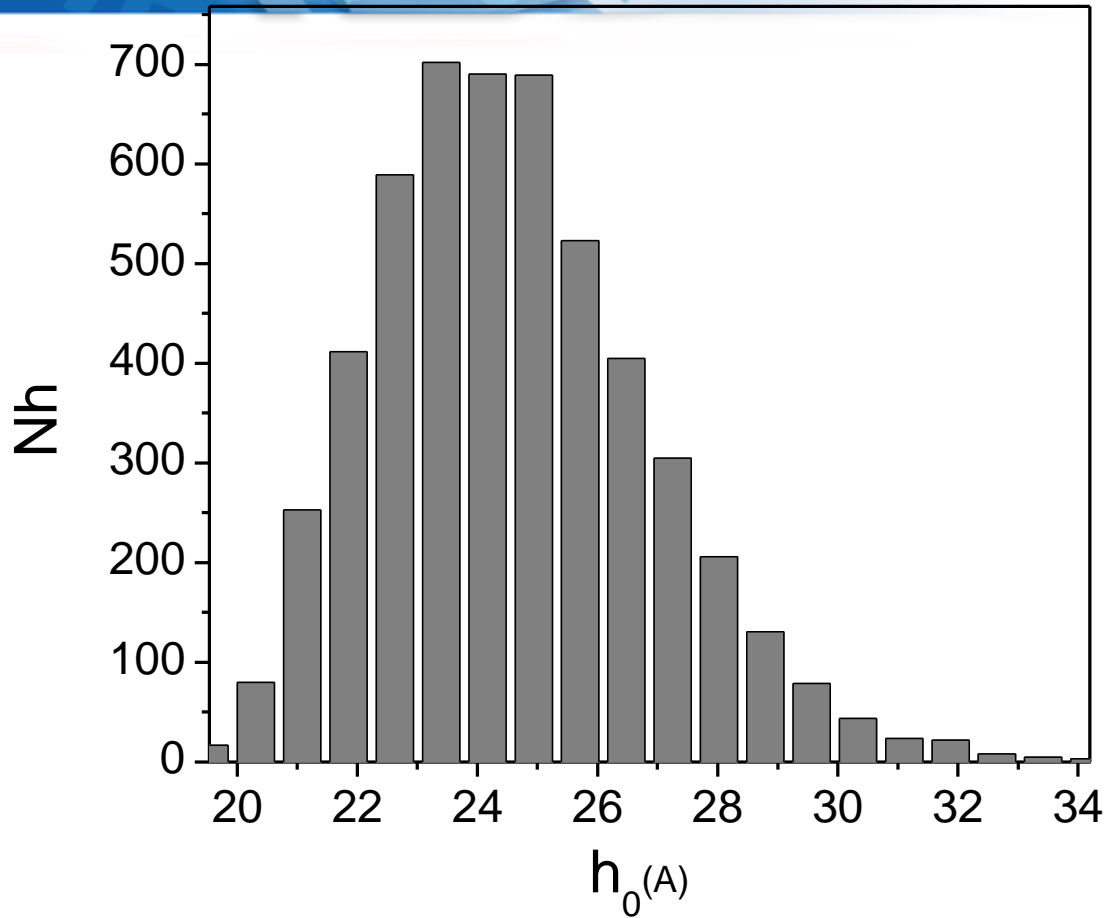
ZnTe QD



Photoluminescence spectra of the ZnTe QDs with coverage of 2.5, 3.0, 3.5, and 4.0 MLs.



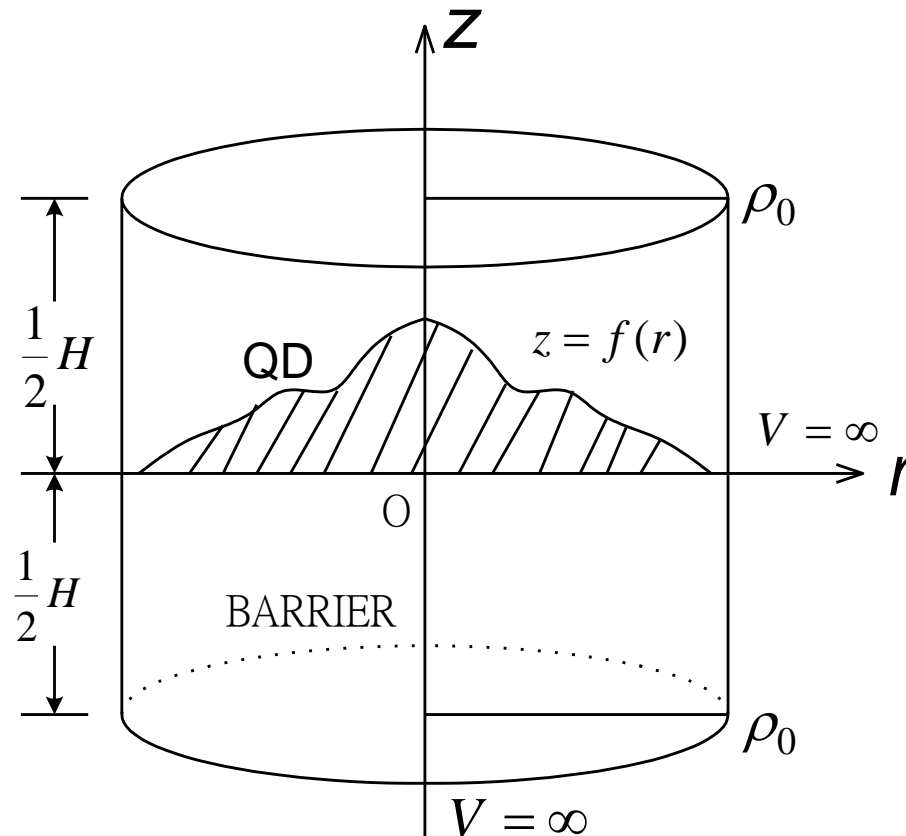
Dot size distribution: number of QDs N_{QD} versus base diameter D and height h_0 in \AA measured by AFM. There are 5187 dots in an area of $3 \times 3 \mu\text{m}^2$.



Histogram of number N_h versus h_0 . N_h is a sum of the number of dots over all possible D 's with the same height h_0 .



collaborator: **Dr. Johnson Lee (theoretical calculations)**



$$\Psi_{nml}(\mathbf{r}, \varphi, z) = R_{nm}(\mathbf{r}) Z_1(z) \Phi_m(\varphi)$$

$$R_{nm}(\mathbf{r}) = \frac{\sqrt{2}}{\rho_0 J_{m+1}(k_n \rho_0)} J_m(k_n r), \quad 0 \leq r \leq \rho_0$$



H

$\Delta E_C \sim 0.315 \text{ eV}$

2.085 eV

$\Delta E_V \sim 0.735 \text{ eV}$

ZnSe ZnTe ZnSe

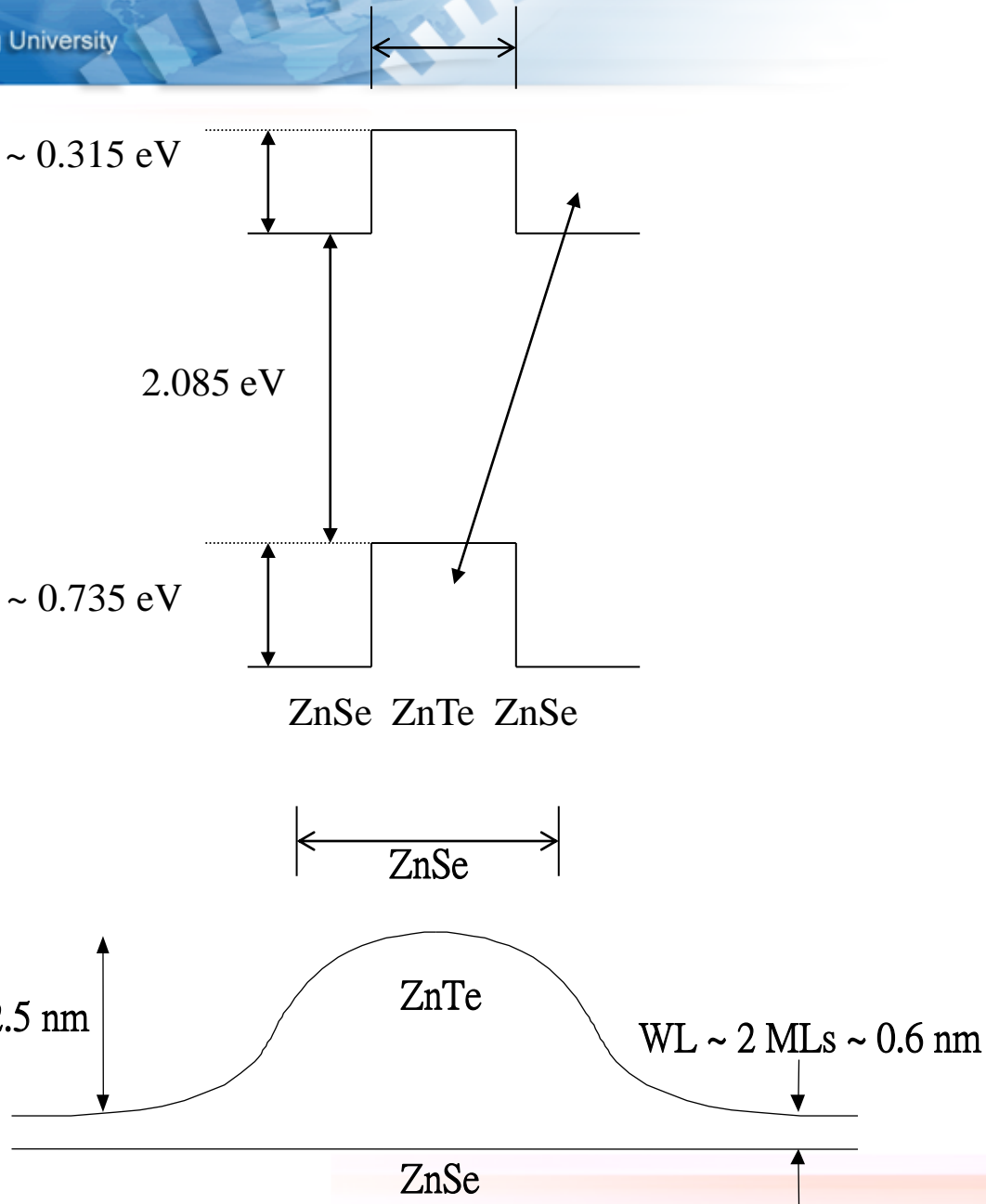
ZnSe

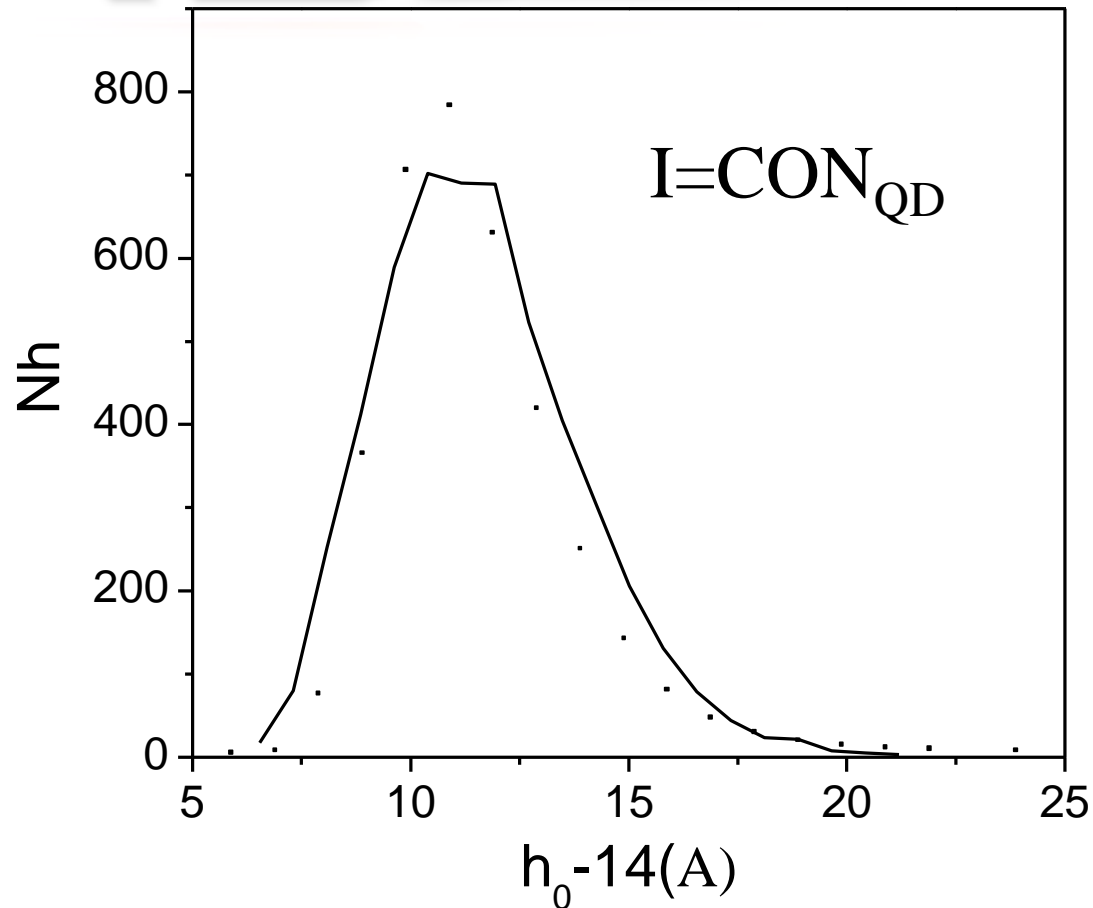
H ~ 2.5 nm

ZnTe

WL ~ 2 MLs ~ 0.6 nm

ZnSe

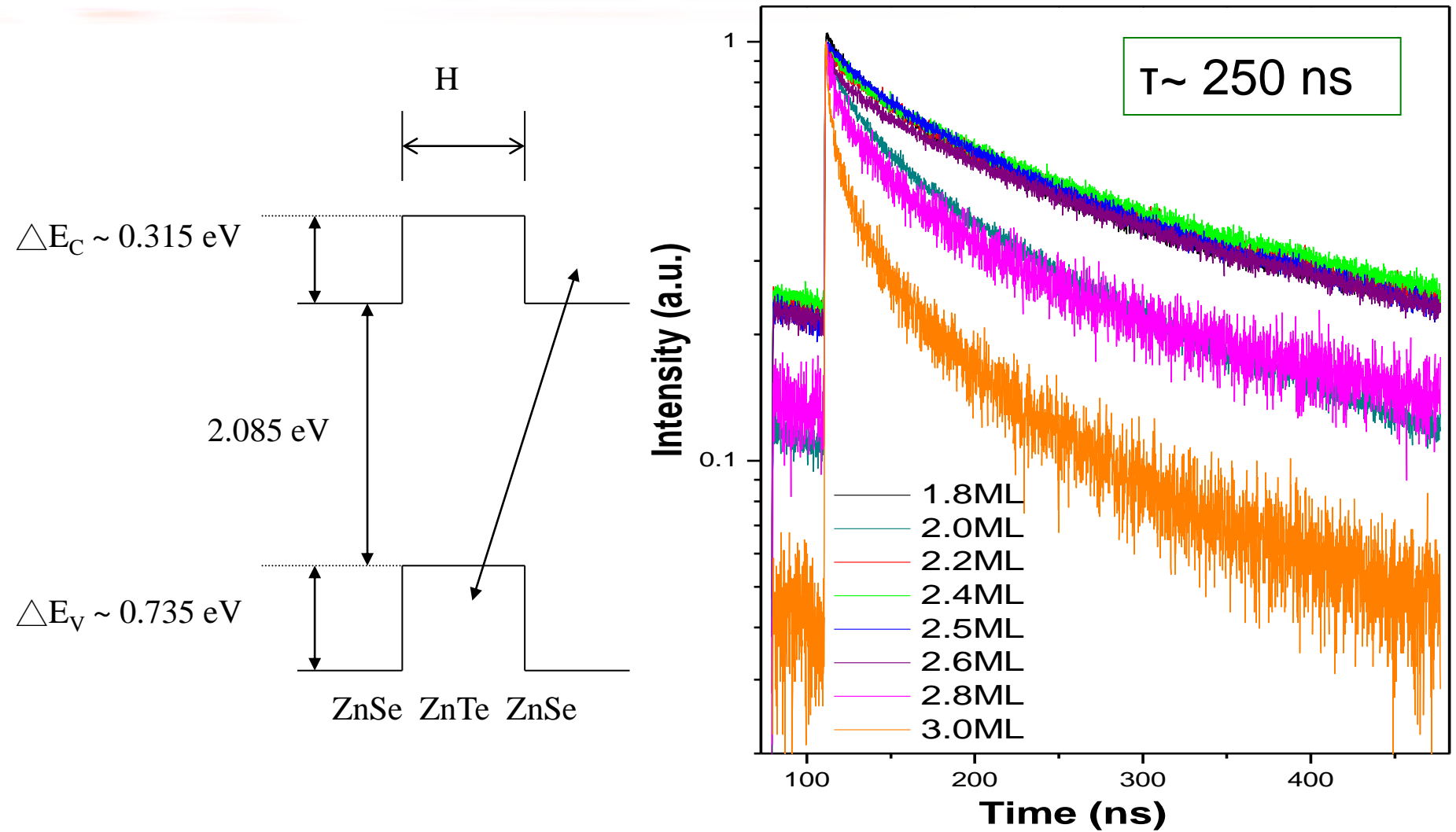




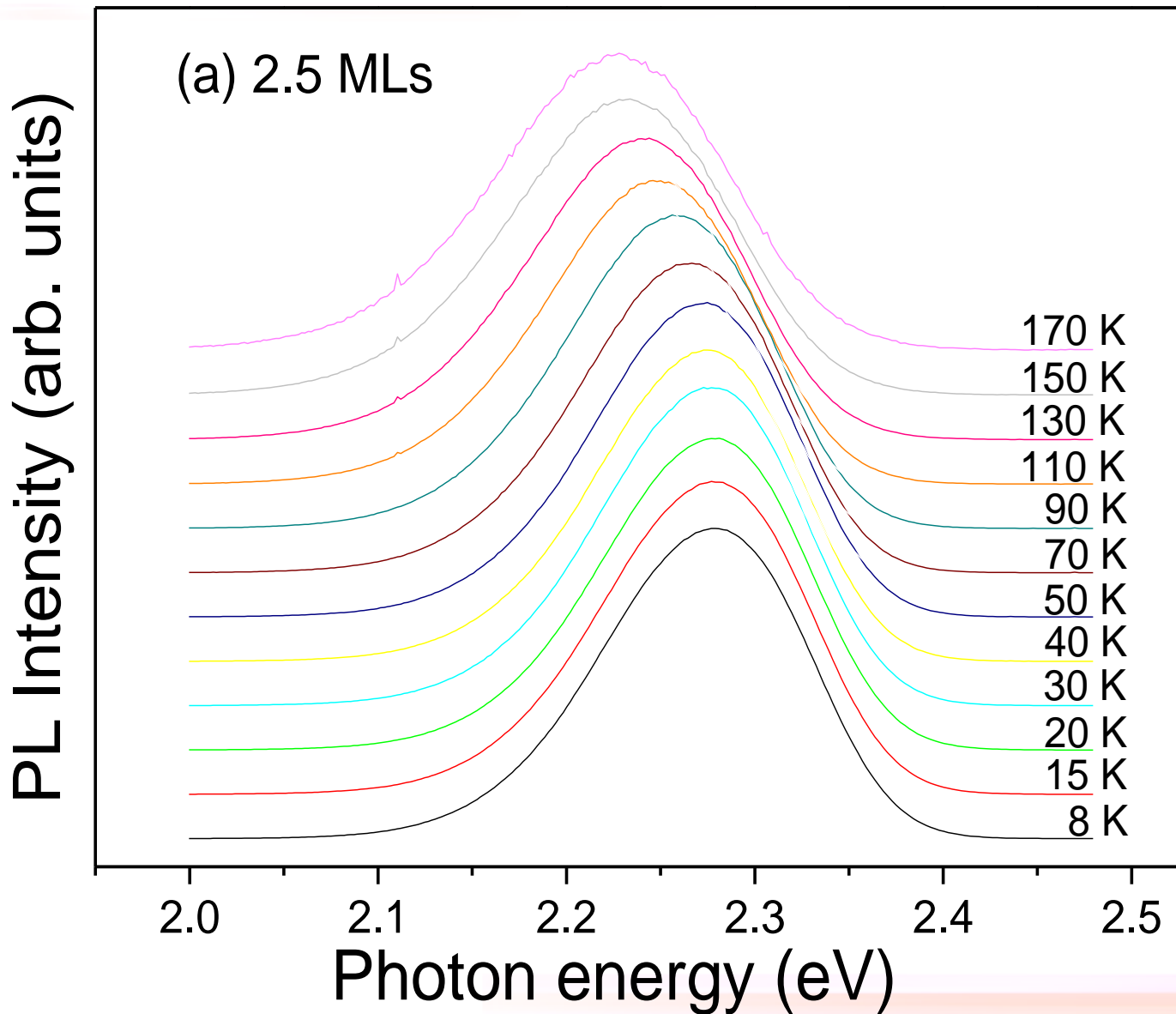
Solid curve: AFM measurement N_{QD}

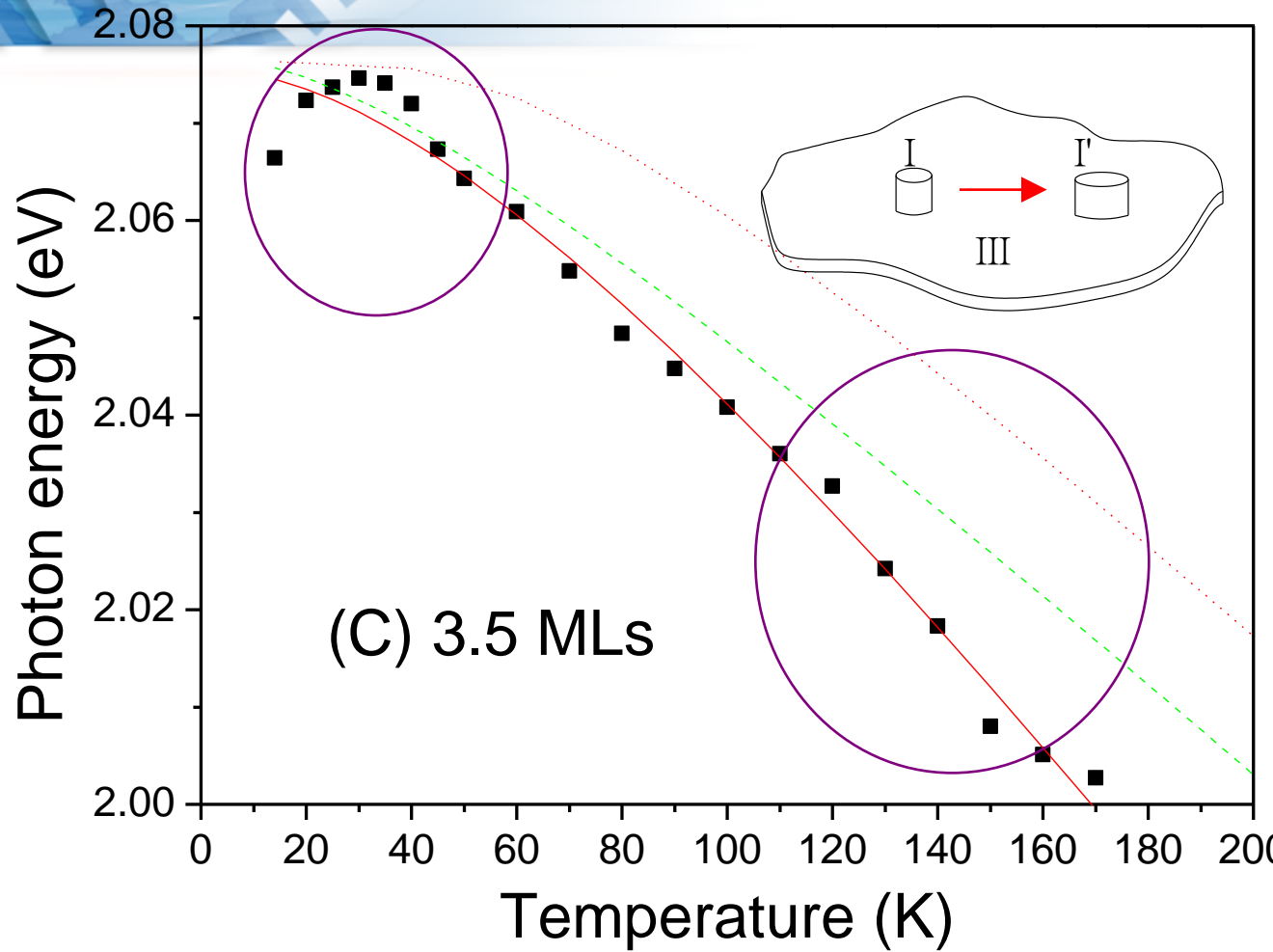
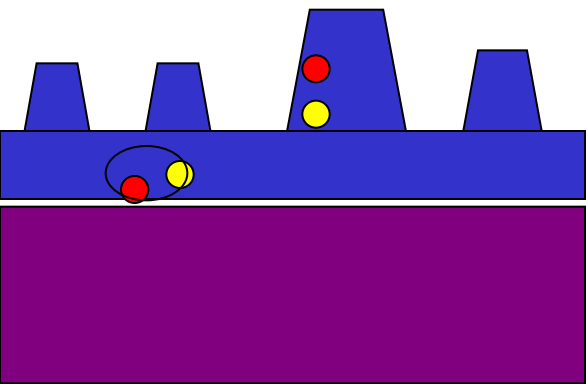
Dots: theoretical calculations

C is an arbitrary constant. O is the overlap integral.

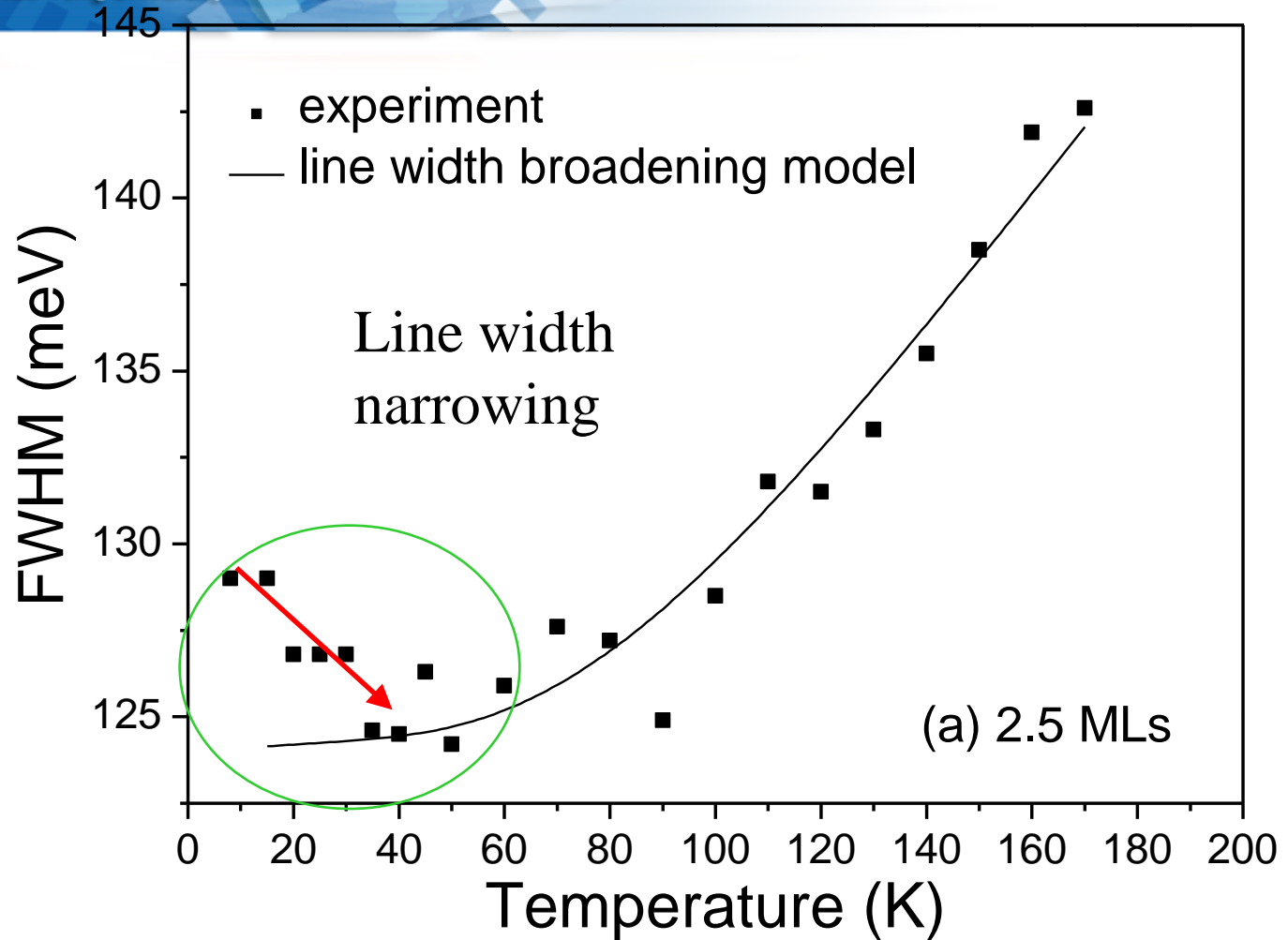


Long lifetime is a signature of type II emission





Signature of carrier transfer between smaller dot - wetting layer - larger dot. **Initial blue shift at low T**, then **a fast red shift**. The red-shift is about 0.5 meV/K for QD and is much larger than that of ZnTe epilayer of roughly 0.35 meV/K.



Solid curve is obtained by the fit:

$$\Gamma(T) = \Gamma_0 + \Gamma_a T + \Gamma_{LO} / [\exp(\hbar\omega_{LO} / kT) - 1] + \Gamma_i \exp(-\langle E_b \rangle / kT)$$



Single-electron charging of a self-assembled II–VI quantum dot

J. Seufert,^{a)} M. Rambach, G. Bacher, and A. Forchel

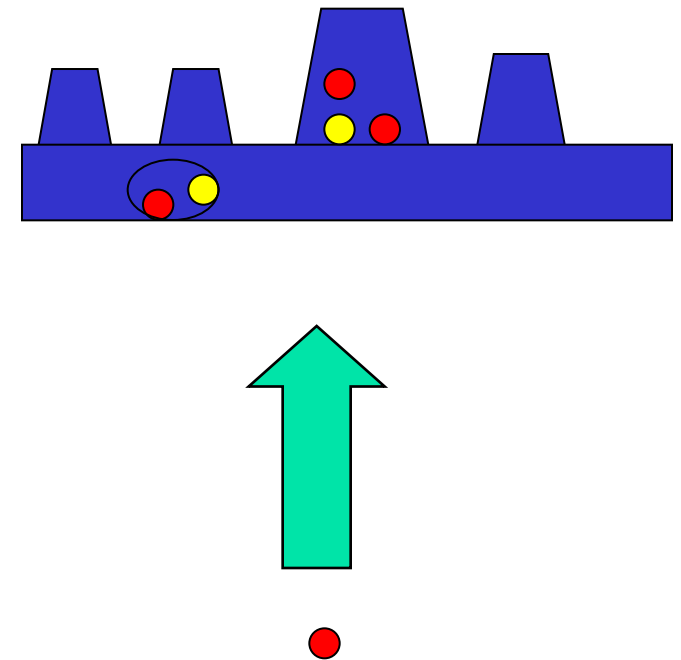
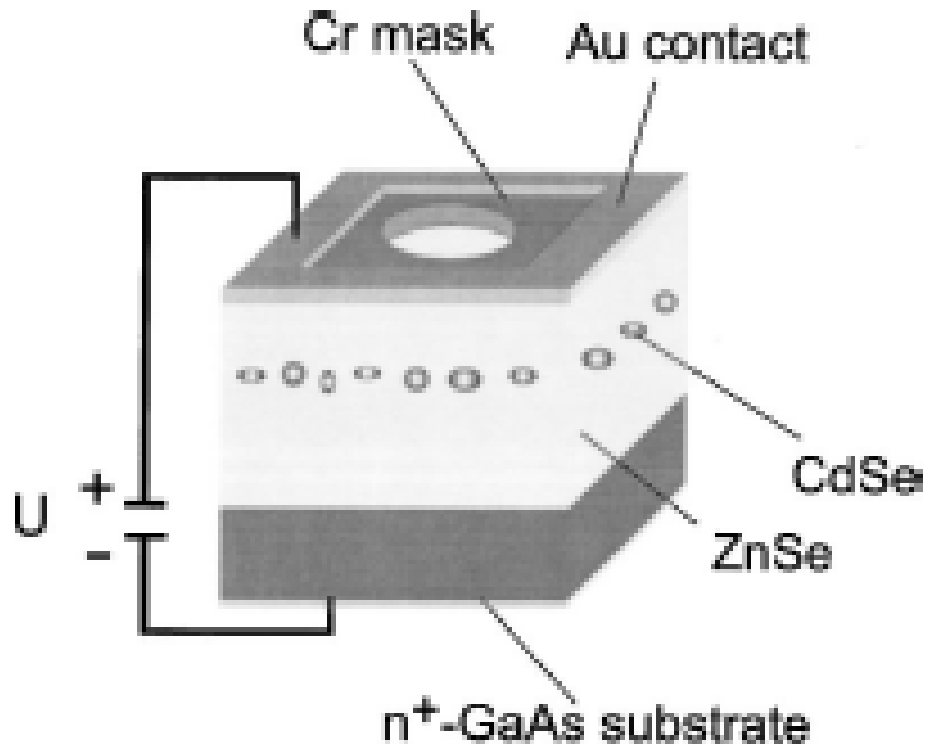
Technische Physik, Universität Würzburg, Am Hubland, D-97074 Würzburg, Germany

T. Passow and D. Hommel

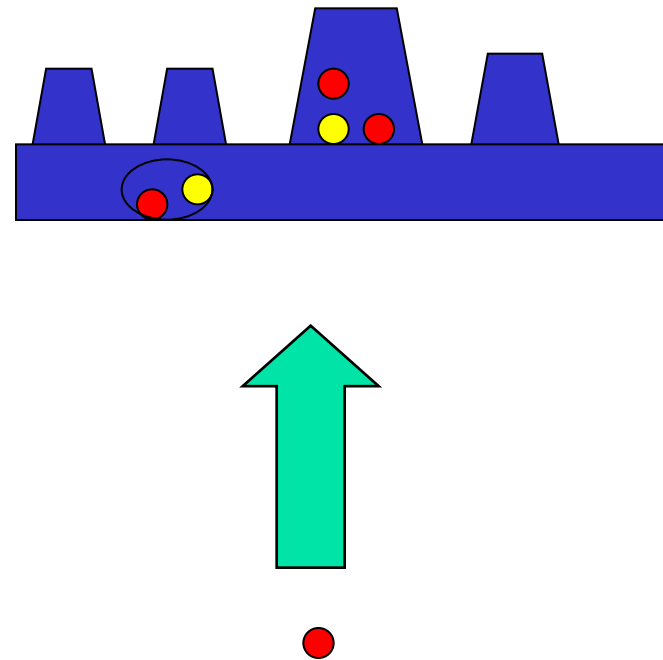
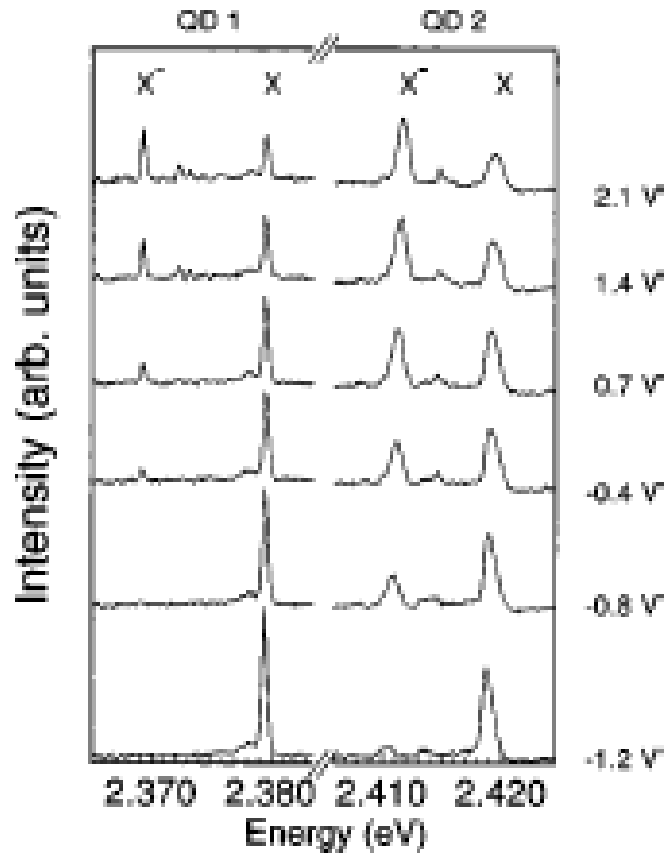
Institut für Festkörperphysik, Universität Bremen, D-28359 Bremen, Germany

APL v82, 3946 (2004)

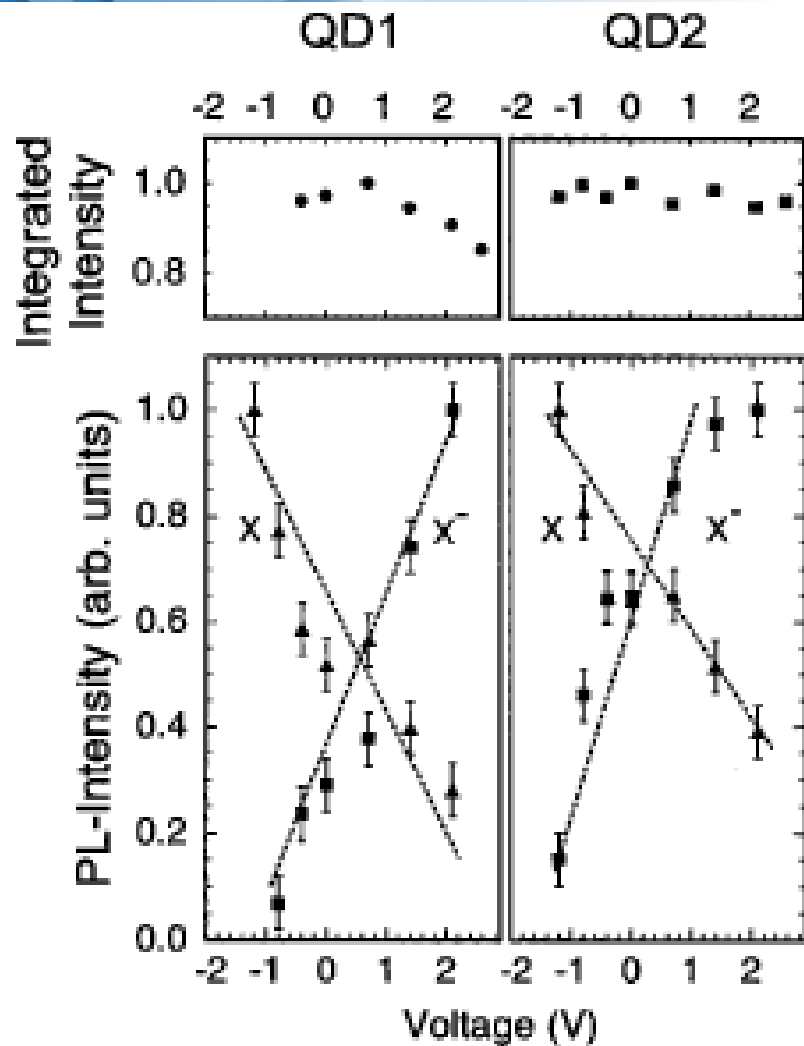
We have studied single-electron injection into individual self-assembled CdSe/ZnSe quantum dots. Using nanostructured contacts to apply a vertical electric field, excess electrons are promoted to the single-quantum-dot ground state in a controlled fashion. Spatially-resolved photoluminescence spectroscopy is applied to demonstrate single-quantum-dot charging via the formation of single zero-dimensional charged excitons with a binding energy on the order of 10 meV.



Schematic representation of the sample design for the spectroscopy of single quantum dots in a vertical electric field.



PL spectra of two individual QDs ~QD1 and QD2! obtained using a nanoaperture of diameter 200 nm for various values of an applied bias voltage. Single luminescence lines labeled as X (X2) correspond to the emission from the neutral ~charged! exciton transition.



Bottom: PL intensities of the neutral and the charged exciton transition in two single QDs as a function of the applied voltage. Top: Summarized intensity of the neutral and charged exciton transition for each QD.



Near-Field Optical Mapping of Exciton Wave Functions in a GaAs Quantum Dot

K. Matsuda,^{1,2,*} T. Saiki,^{1,3} S. Nomura,^{4,5} M. Mihara,⁵ Y. Aoyagi,^{5,6} S. Nair,⁷ and T. Takagahara⁸

PRL v91, 177401 (2003)

Near-field photoluminescence imaging spectroscopy of naturally occurring GaAs quantum dots (QDs) is presented. We successfully mapped out center-of-mass wave functions of an exciton confined in a GaAs QD in real space due to the enhancement of spatial resolution up to 30 nm. As a consequence, we discovered that the spatial profile of the exciton emission, which reflects the shape of a monolayer high island, differs from that of biexciton emission, due to different distributions of the polarization field for the exciton and biexciton recombinations. This novel technique can be extensively applied to wave function engineering in the design and the fabrication of quantum devices.

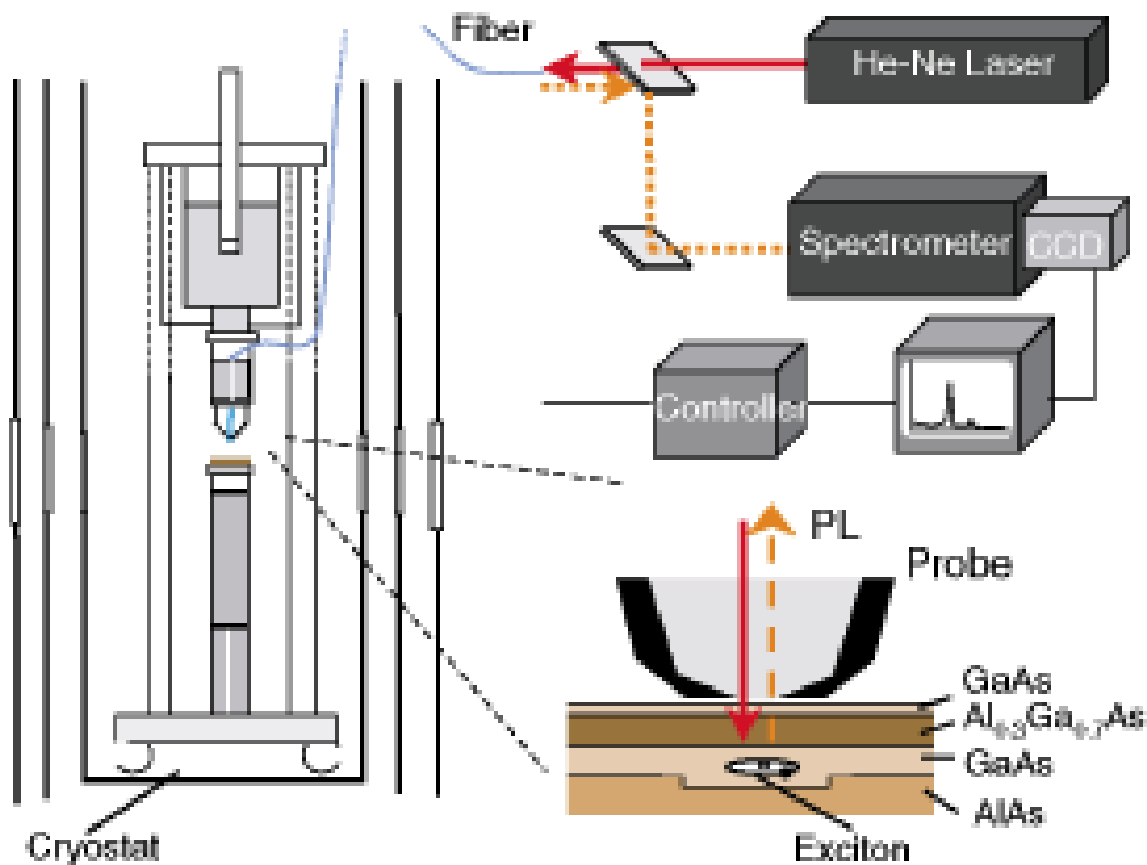
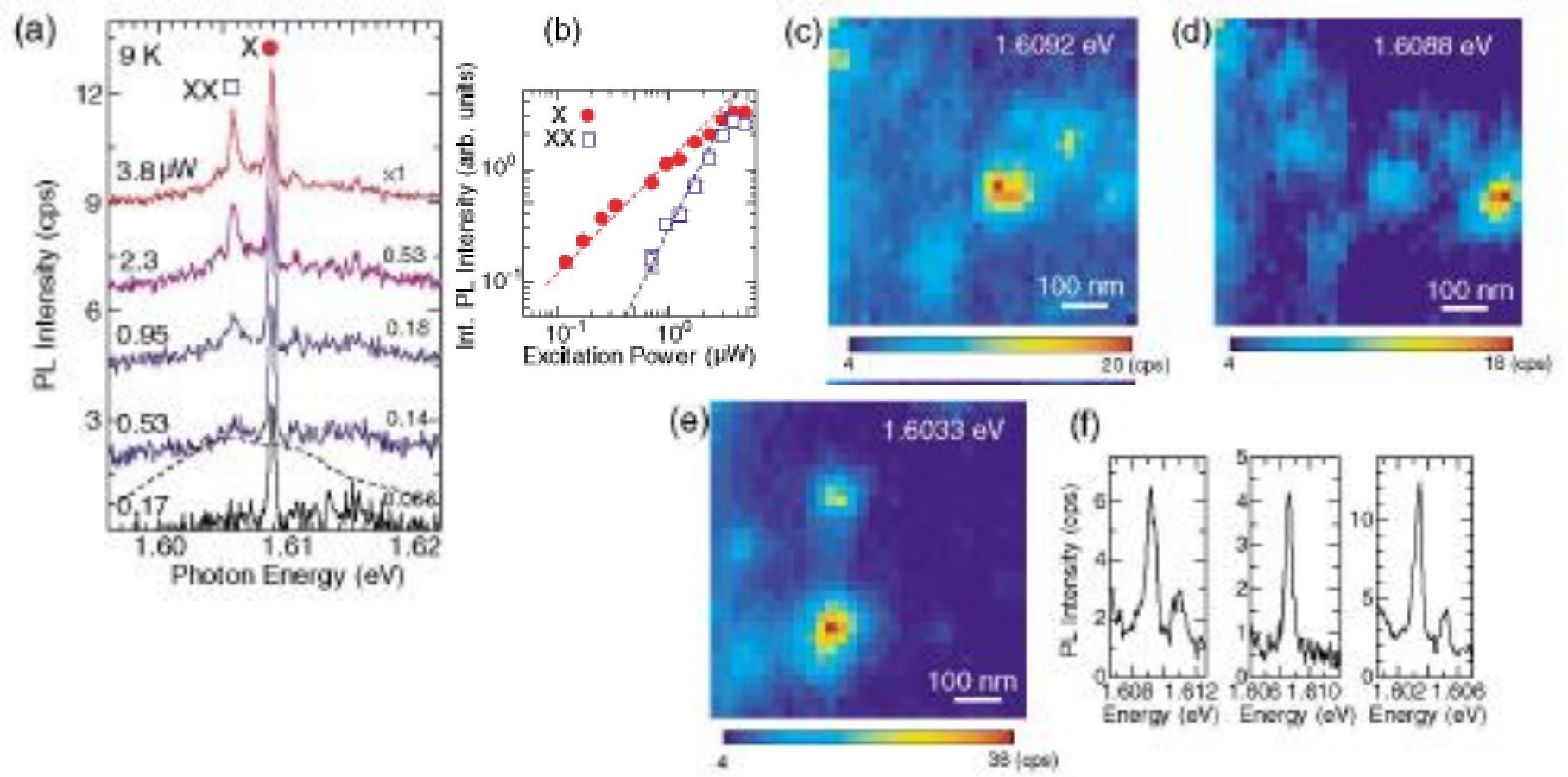
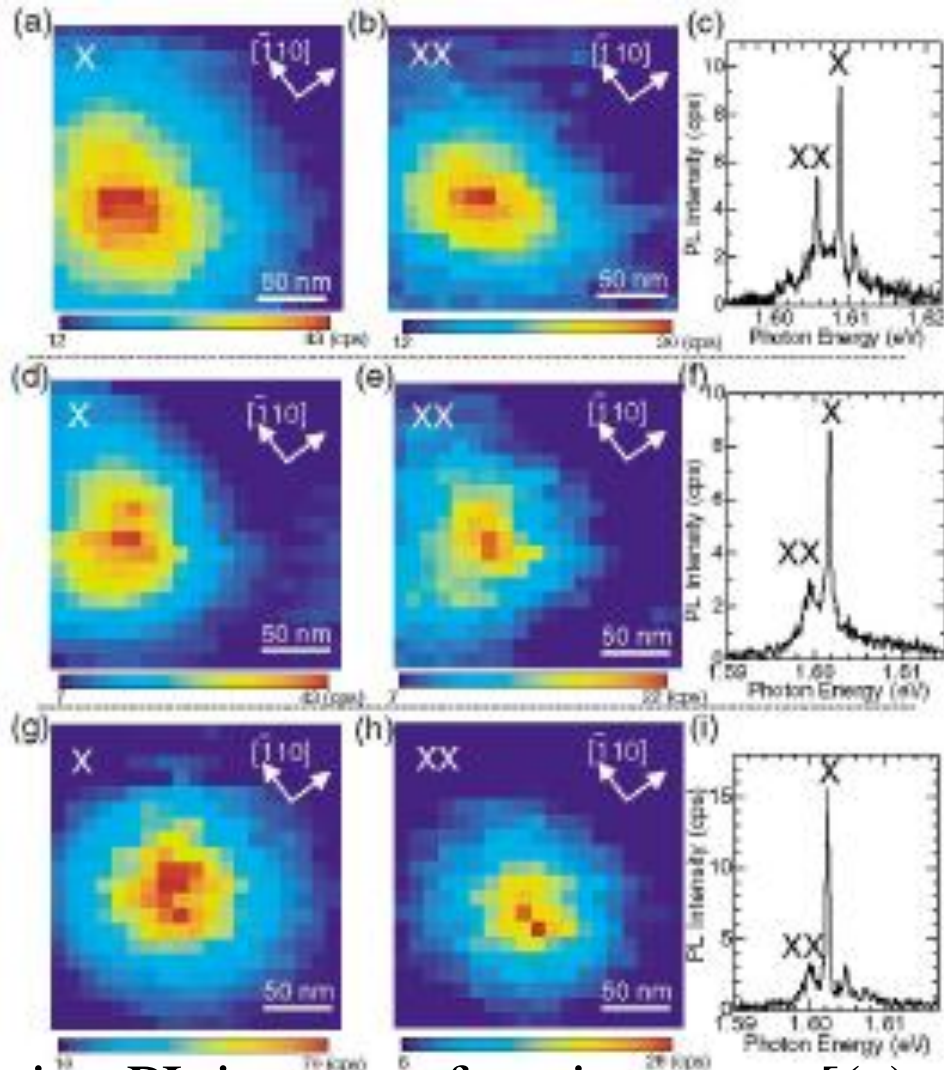


FIG. 1 (color). Schematic of low temperature near-field scanning optical microscope and experimental setup of near-field photoluminescence (PL) measurement. Sample structures of naturally occurring quantum dot (QD) in a narrow quantum well and the near-field probe are shown.



Near-field PL spectra of a single QD (solid lines) and far-field PL spectrum (dotted line) at 9 K (a). The PL peaks at 1.6088 and 1.6057 eV are denoted by X and XX. Excitation power dependence of integrated PL intensities of the X and the XX lines (b). The red (blue) dotted line corresponds to the gradient associated with linear (quadratic) power dependence. Near-field PL images obtained by mapping the intensity of the X lines in a same scanning area (1000 1000 nm²) (c) –(e). The PL spectra for generating each image are indicated (f). The QDs in (c) and (d) are in one-monolayer thinner regions and the one in (e) is in a one-monolayer thicker region.



(a) –(i) Series of high-resolution PL images of exciton state [(a), (d), and (g)], biexciton state [(b), (e), and (h)], and corresponding PL spectra [(c), (f), and (i)] for three different QDs. Scanning area is $210 \times 210 \text{ nm}^2$. Crystal axes along 110 and $\bar{1}\bar{1}0$ directions are indicated. PL image sizes of biexciton are always smaller than those of exciton.